Biochemical and Biophysical Research Communications 461 (2015) 671–676

Contents lists available at ScienceDirect

Biochemical and Biophysical Research Communications

journal homepage: www.elsevier.com/locate/ybbrc

Locomotion of bacteria in liquid flow and the boundary layer effect on bacterial attachment

Chao Zhang [a, b], Qiang Liao [a, b, *], Rong Chen [a, b], Xun Zhu [a, b]

[a] Key Laboratory of Low-grade Energy Utilization Technologies and Systems (Chongqing University), Ministry of Education, Chongqing 400030, China
[b] Institute of Engineering Thermophysics, Chongqing University, Chongqing 400030, China

ARTICLE INFO

Article history:
Received 3 April 2015
Available online 24 April 2015

Keywords:
Biofilm
Bacteria
Locomotion
Attachment
Boundary layer
Liquid flow

ABSTRACT

The formation of biofilm greatly affects the performance of biological reactors, which highly depends on bacterial swimming and attachment that usually takes place in liquid flow. Therefore, bacterial swimming and attachment on flat and circular surfaces with the consideration of flow was studied experimentally. Besides, a mathematical model comprehensively combining bacterial swimming and motion with flow is proposed for the simulation of bacterial locomotion and attachment in flow. Both experimental and theoretical results revealed that attached bacteria density increases with decreasing boundary layer thickness on both flat and circular surfaces, the consequence of which is inherently related to the competition between bacterial swimming and the non-slip motion with flow evaluated by the Péclet number. In the boundary layer, where the Péclet number is relatively higher, bacterial locomotion mainly depends on bacterial swimming. Thinner boundary layer promotes bacterial swimming towards the surface, leading to higher attachment density. To enhance the performance of biofilm reactors, it is effective to reduce the boundary layer thickness on desired surfaces.

1. Introduction

Immobilized cell systems have become common alternatives to suspended cell systems in continuous operations since they are more efficient in solid/liquid separation and can be operated at low retention times without encountering washout of cells. Among existing immobilized systems, biofilm based biological system is typical. Basically, biofilm can be defined as a well-organized, cooperating community of microorganisms, which has been widely used in many fields such as biochemical treatment of wastewater, hydrogen production and biological conversion of gaseous compound [1–3]. Obviously, the performances of these biological systems are critically dependent of the biofilm, which is affected by biofilm formation. As a result, it is essential to investigate the characteristics of the biofilm formation.

In general, the formation of biofilm undergoes four subsequent steps: swimming bacteria in suspension, initial attachment, irreversible attachment, maturation and dispersion. Among the four steps, swimming of bacteria and their attachment on surfaces greatly affect the formation of biofilm, and then determine the performance of the biological reactor. It has been known that bacterium swims by rotating its helical shaped flagella embedded in the cell body, while the cell body rotates in the opposite direction. Peritrichous bacteria such as *Escherichia coli* have several flagella, while the others are monotrichous with single flagella. The peritrichous bacteria have two types of motion: running (motion in approximately straight paths) and tumbling (spinning in place for a certain period). Besides self-propulsion, the motion of bacterium is also altered by constant thermal agitation known as Brownian motion [4]. Particularly, Brownian motion is of fundamental significance for microbial life, especially for the monotrichous bacteria. However, existing study of biofilm formation are mainly concentrated on the adhesion process and biofilm growth by experimental observation or numerical simulation [5,6]. The influences of bacterial swimming in biofilm formation are rarely discussed and studied.

Besides, it should be pointed out that the bacterial attachment and biofilm formation usually take place in fluid flow. Biofilm formation and bacteria accumulation in the fluid flow between porous matrices was studied by experimental observation [7]. It was revealed that the bacteria distribution is affected by the geometry.

* Corresponding author. Institute of Engineering Thermophysics, Chongqing University, Chongqing 400030, China. Fax: +86 23 65102474.
E-mail addresses: zhangchao@cqu.edu.cn (C. Zhang), lqzx@cqu.edu.cn (Q. Liao), rchen@cqu.edu.cn (R. Chen), zhuxun@cqu.edu.cn (X. Zhu).

http://dx.doi.org/10.1016/j.bbrc.2015.04.089
0006-291X/

Moreover, modelling the effects of dispersal mechanisms and hydrodynamic regimes upon the structure of microbial communities was also performed [8]. However, bacterial swimming in fluid flow, especially in terms of biofilm formation, has been rarely reported.

The above literature review indicates that the influence of the bacterial locomotion with the consideration of the fluid flow has not been yet reported. In the present study, therefore, an experimental platform is designed to study the bacterial attachment in fluid flow with various velocity profiles. We also propose a comprehensive model combining flagellar propulsion, Brownian motion, tumbling and the motion with flow to simulate the bacterial locomotion and attachment under the fluid flow environment. The results obtained in this work can be used as a guideline for the design and optimization of biological reactor.

2. Materials and methods

2.1. Experiment

The ingredients for the bacterial culture medium are (per liter distilled water): $Na_2HPO_4 \cdot 12H_2O$ 15.35 g; KH_2PO_4 3 g; $CH_3COONa \cdot 3H_2O$ 1.1285 g; NaCl 0.5 g; NH_4Cl 0.1 g; $MgSO_4 \cdot 7H_2O$ 0.1 g; $CaCl_2$ 11.327 mg, and 1 ml of trace element solution. The trace element solution contains (per liter): $FeSO_4 \cdot 7H_2O$ 1 g; $ZnCl_2$ 70 mg; $MnCl_2 \cdot 4H_2O$ 100 mg; H_3BO_3 6 mg; $CaCl_2 \cdot 6H_2O$ 130 mg; $CuCl_2 \cdot 2H_2O$ 2 mg; $NiCl_2 \cdot 6H_2O$ 24 mg; $Na_2Mo_4 \cdot 2H_2O$ 36 mg; $CoCl_2 \cdot 6H_2O$ 238 mg. Following high temperature sterilization, the culture medium was cooled down to room temperature. *E. coli* was then inoculated with the culture medium and stored in a flask. The experimental system is shown in Fig. 1A. The bacteria suspension was delivered from the flask to the bioreactor continuously by a peristaltic pump (YZ1515, Tianjin Xieda Exectron Co., Ltd.) with constant flow rate. The bioreactor was fabricated using polymethylmethacrylate (PMMA). As shown in Fig. 1B, two plates with one chamber in the middle were assembled. Rectangular obstructions with the dimension of 60 mm × 20 mm × 10 mm and cylindrical obstructions with the dimension of 20 mm × ϕ10 mm were located in the chamber to obtain various velocity profiles of the fluid flow (Fig. 1C and D). To prevent entrance effect and exit effect, they were located in the central section of the reactor.

After 12 days of continuous running with constant flow rate of 180 mL/min for each bioreactor, they were disassembled and the obstructions were observed under phase contrast microscope. For quantitative analysis, the number of attached bacteria on the surface of the obstructions is counted by microscopic examination and the bacterial density is calculated in the way of cells/mm^2. For the rectangular obstruction, the surface with the dimension of 60 mm × 20 mm was observed. While for the cylindrical obstruction, the circular surface was observed.

2.2. Mathematical model

The mathematical model for bacterial locomotion in flow takes four factors into consideration: flagellar propulsion, Brownian motion, tumbling and the motion with fluid flow. In the following the four factors are expatiated separately.

2.2.1. Flagellar propulsion

For the simulation of flagellar propulsion, resistive force theory is adopted since the Reynolds number for a swimming bacteria in liquid is small enough due to its dimension [9–11]. The resistive force theory assumes that the local body velocity relative to the

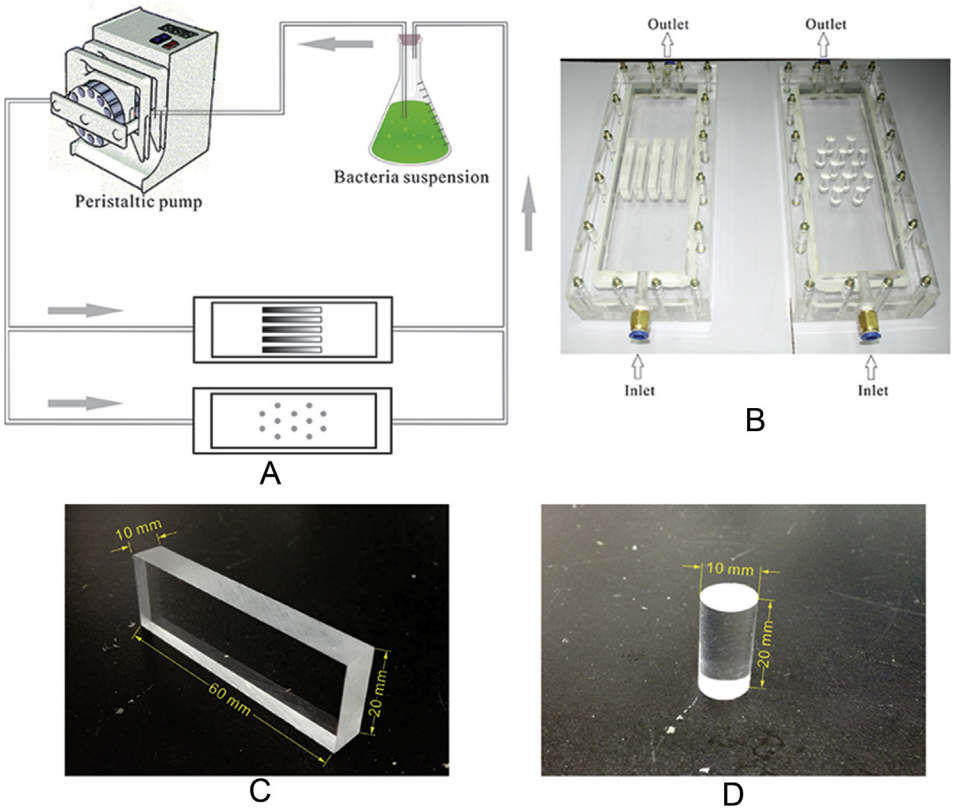

Fig. 1. Experimental platform for bacterial swimming and attachment in fluid flow. (A) Schematic of the experimental platform, (B) image of the bioreactor, (C) image of the rectangular obstruction, (D) image of the cylindrical obstruction.

ambient fluid is proportional to the hydrodynamic forces applied on it, with the constant of proportionality defined as viscous mobilities [10,11]. The bacterium chosen in this model is *E. coli*, which has been a common model organism for the study of bacterial motile behavior [12]. Note that this model is applicable to both peritrichous and monotrichous bacteria with reasonable accuracy [13]. The velocity of the bacterium by flagellar propulsion is calculated as:

$$U_x \approx \frac{W_{zy}^{L\Omega}}{\left(\frac{M_{zz}^{L\Omega}\left(M_{xx}^{FU}+N_{xx}^{FU}\right)}{M_{xz}^{F\Omega}} - M_{zx}^{LU}\right)}\omega \tag{1}$$

$$U_y \approx \frac{M_{yy}^{F\Omega}}{M_{yy}^{FU}+N_{yy}^{FU}}\omega \tag{2}$$

$$U_z \approx -\frac{V_{xy}^{LU}M_{zx}^{F\Omega}M_{yy}^{F\Omega}}{N_{zz}^{FU}M_{xx}^{L\Omega}\left(M_{yy}^{FU}+N_{yy}^{FU}\right)}\omega \tag{3}$$

In which M and N are the viscous mobilities of the flagella and cell body, respectively. They are related to the shape and dimension of the bacteria. W and V are the mobilities derived from the solid surface. ω is the rotation rate of the flagella. For all these mobilities (e.g. $M_{ij}^{\alpha\beta}$), ij denotes how the ith component of a viscous force is linearly related to the jth component of the cell velocity ($F_i = M_{ij}^{FU}U_j$), $F\Omega$ (relation between force and rotation rate), LU (relation between torque and velocity), or $L\Omega$ (relation between torque and rotation rate). The calculations of these mobilities are referred to the study by E. Lauga et al. [14].

2.2.2. Brownian motion

For Brownian motion, the random displacement of the bacteria can be calculated as:

$$<x^2>^{1/2} = (2D_t\Delta t)^{1/2} \tag{4}$$

"< >" denotes for an average over time and over an ensemble of bacteria in the simulation. $<x^2>^{1/2}$ is the root-mean-square displacement. D_t is the translational diffusion constant characterizes the migration of *E. coli* in a given medium at given temperature [4]. In our model,

$$\Delta x = \alpha\sqrt{2D_t\Delta t} \tag{5}$$

$$\Delta y = \beta\sqrt{2D_t\Delta t} \tag{6}$$

$$\Delta z = \gamma\sqrt{2D_t\Delta t} \tag{7}$$

α, β, γ are Gaussian distributed random numbers with zero mean and unit variance. Δt is the time step. The time step is chosen as a compromise between fast simulation and small error. In our model, $\Delta t = 0.001$ s. The random changes in direction caused by Brownian motion are calculated in a similar way.

2.2.3. Tumbling

In the model, it is assumed that there is no chemical gradient in the fluid flow. So the probability of run and tumble is equal at any point in all directions. The distribution of changes in direction is referred to the experimental observation in Ref. [15]. The scattered tumble angle and its probability is shown in Table 1.

Table 1
Tumble angles and their corresponding probabilities in simulation.

Tumble angle (degree)	Probability
5	0.021441
15	0.048027
25	0.06175
35	0.098628
45	0.114923
55	0.114923
65	0.108919
75	0.078902
85	0.073756
95	0.054031
105	0.048027
115	0.045455
125	0.036878
135	0.03259
145	0.022298
155	0.017153
165	0.013722
175	0.008576

If the velocity of a bacterium $\boldsymbol{U}(U_x, U_y, U_z)$ rotates around a vector $\boldsymbol{P}(P_x, P_y, P_z)$ with an angle θ, then the velocity $\boldsymbol{U'}(U'_x,\ U'_y,\ U'_z)$ after the rotation is:

$$\begin{aligned} U'_x =& U_x\cdot\cos\theta + (P_y\cdot U_z - P_z\cdot U_y)\sin\theta \\ &+ P_x\cdot(P_x\cdot U_x + P_y\cdot U_y + P_z\cdot U_z)(1-\cos\theta) \end{aligned} \tag{8}$$

$$\begin{aligned} U'_y =& U_y\cdot\cos\theta + (P_x\cdot U_z - P_z\cdot U_x)\sin\theta + \\ & P_y\cdot(P_x\cdot U_x + P_y\cdot U_y + P_z\cdot U_z)(1-\cos\theta) \end{aligned} \tag{9}$$

$$\begin{aligned} U'_z =& U_z\cdot\cos\theta + (P_x\cdot U_y - P_y\cdot U_x)\sin\theta + \\ & P_z\cdot(P_x\cdot U_x + P_y\cdot U_y + P_z\cdot U_z)(1-\cos\theta) \end{aligned} \tag{10}$$

2.2.4. Bacterial motion with fluid flow

For incompressible Newtonian fluid, the fluid velocity can be solved with the Navier–Stokes equations:

$$\frac{du_x}{dt} = X - \rho\frac{\partial p}{\partial x} + \nu\left(\frac{\partial^2 u_x}{\partial x^2} + \frac{\partial^2 u_x}{\partial y^2} + \frac{\partial^2 u_x}{\partial z^2}\right) \tag{11}$$

$$\frac{du_y}{dt} = Y - \rho\frac{\partial p}{\partial y} + \nu\left(\frac{\partial^2 u_y}{\partial x^2} + \frac{\partial^2 u_y}{\partial y^2} + \frac{\partial^2 u_y}{\partial z^2}\right) \tag{12}$$

$$\frac{du_z}{dt} = Z - \rho\frac{\partial p}{\partial z} + \nu\left(\frac{\partial^2 u_z}{\partial x^2} + \frac{\partial^2 u_z}{\partial y^2} + \frac{\partial^2 u_z}{\partial z^2}\right) \tag{13}$$

In which u_x, u_y and u_z are the fluid velocity, X, Y, Z are the mass forces, ρ is the density of the fluid, p is the pressure of the fluid, ν is the kinematic viscosity. We use COMSOL Multiphysics to solve the Navier–Stokes equations. In the model, the inlet and outlet are set as constant flow rate boundary. All other boundaries are treated as non-slip boundary. For bacterial motion with flow, the Reynolds number for a swimming bacterium is very small, therefore it is reasonable to assume that there is no slip velocity between the bacterium and its ambient fluid. For a bacterium with the swimming velocity U_b, if the fluid velocity to the bioreactor at the location of the bacterium is $U_f(u_x, u_y\ u_z)$, then the total velocity of the bacterium to the bioreactor is:

$$U_{total} = U_b + U_f \quad (14)$$

In the simulation, all the four factors introduced above are calculated and combined in each time step. By such means we can simulate the locomotion of bacteria in fluid flow.

3. Results and discussions

The rectangular obstruction was observed under phase contrast microscope after 12 days of continuous running. Attached bacteria with different distances to the inlet was examined, since the velocity profile between two parallel plates varies due to entrance and exit effect. The number of attached bacteria is also counted and the density is calculated. Non-uniform bacterial attachment is obtained from the inlet to the outlet of the channel. The attached bacteria at the inlet section has the highest density of 199 cells/mm^2 (Fig. 2A). As a comparison, the attached bacteria at the central section has a lower density, which is 143 cells/mm^2. While for the outlet section, the attached bacteria has the lowest density, which is only 97 cells/mm^2. This non-uniform distribution indicates the entrance is propitious to bacterial attachment. The reason is the entrance effect changes the velocity profile of the flow. As a consequence, it is beneficial for biofilm reactor, since its performance is depended on the biofilm formation on the substratum.

To validate the mathematical model proposed above and confirm that various velocity profiles lead to different bacterial distribution, a simulation of bacterial locomotion with the consideration of fluid flow between two parallel plates was carried out. At the beginning of the simulation, bacteria swim in the flow with uniform distribution (Fig. 2E). The liquid flows over the obstruction, during which some bacteria swim towards the obstruction and attach on it. With elapsed time, bacteria attached on the substratum show non-uniform distribution. The simulation result shows that the entrance section has a higher attached bacteria density compared to the fully developed section and exit section, which is consistent with the experimental observation.

The bacteria attached on the cylindrical obstruction is also observed under microscope. Four positions with various angles to the flow direction were chosen. They were marked as $\theta = 0°$, $\theta = 45°$, $\theta = 90°$ and $\theta = 135°$, separately (Fig. 3). For the position

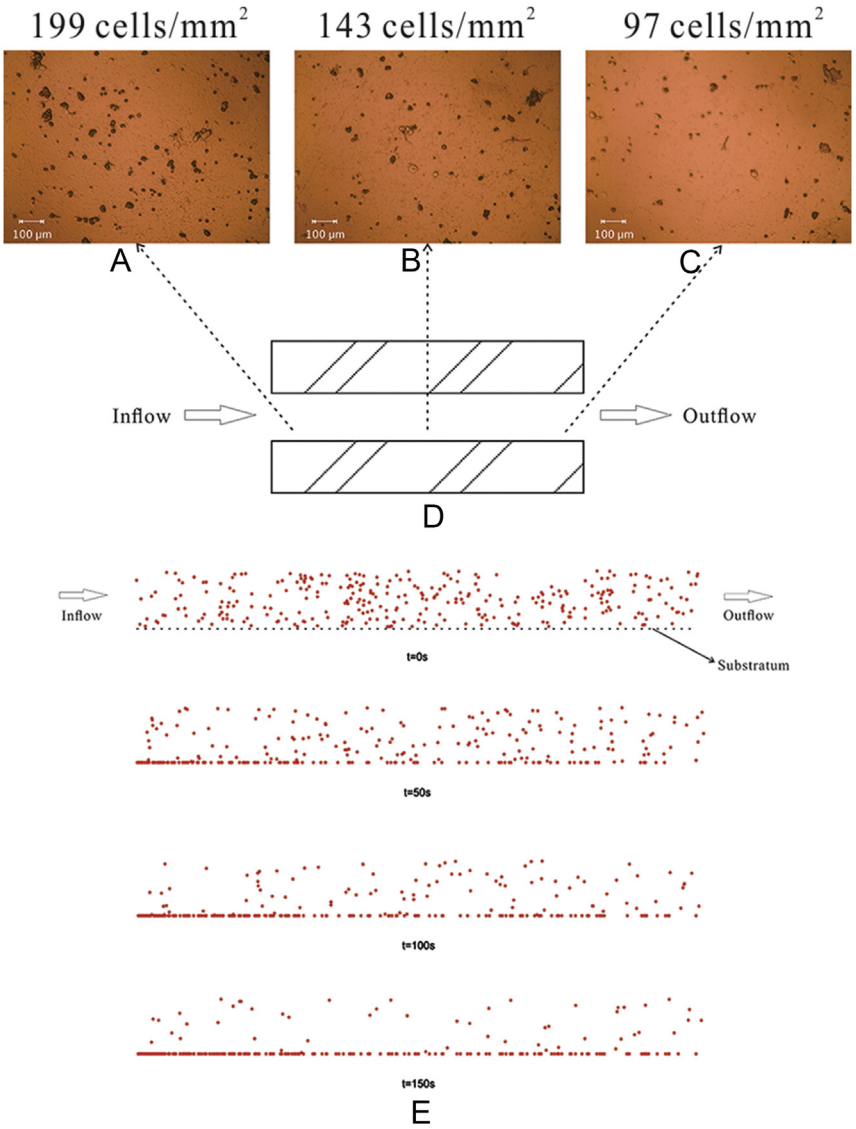

Fig. 2. Attachmed bacteria and their density on the surface of rectangular obstruction. (A) Attached bacteria on the entrance section, (B) central section, (C) the exit section, (D) simulation of bacterial swimming and attachment in rectangular channel.

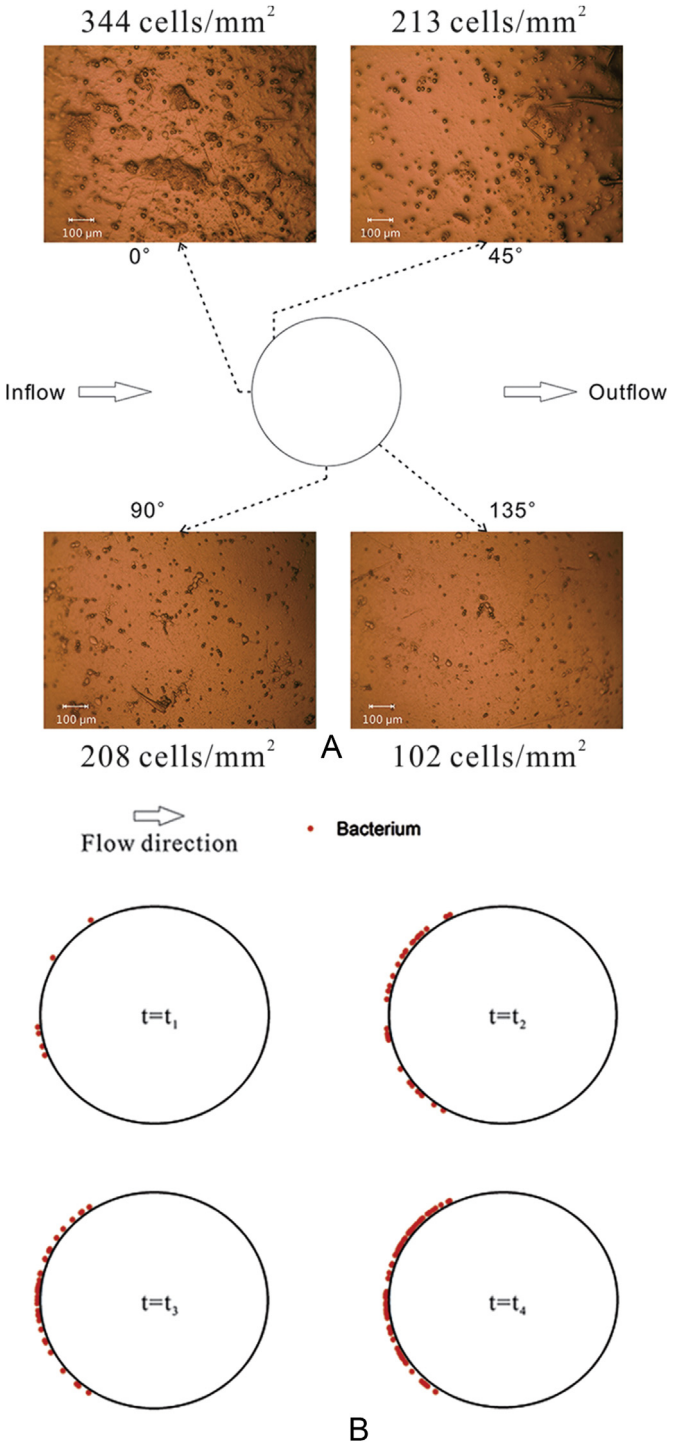

Fig. 3. Attachment bacteria and their density on cylindrical surface. (A) Attached bacteria at the location of $\theta = 0°$, $\theta = 45°$, $\theta = 90°$ and $\theta = 135°$ (B) Simulation of bacterial attachment and attachment on circular surface.

$\theta = 0°$, it is found that the bacteria attached has a highest density, which is 344 cells/mm^2. Some of the bacteria stick to each other with extracellular polymeric substances (EPS). This is an early stage in biofilm formation. Biofilm growth will take place if the bioreactor continues running. As a comparison, the location $\theta = 45°$ has a smaller bacteria density and less bacteria colony. The calculated bacterial density at this location is 213 cells/mm^2. While for the location $\theta = 90°$, no visible bacteria colony is formed. The bacteria density is 208 cells/mm^2, which is close to the location of $\theta = 45°$. However, the sizes of the attached bacteria is smaller compared to the locations $\theta = 0°$ and $\theta = 45°$. This indicates the biofilm formation will be restrained at the location of $\theta = 90°$. For the location $\theta = 135°$, there are even less bacteria attached on the circular surface compared to other three locations. The observed bacteria density is only 102 cells/mm^2.

Based on the mathematical model proposed above, attachment of bacteria on circular surface is also simulated (Fig. 3B). In the simulation, bacterial suspension with uniform bacteria density enters from left and exits from the right. Cylindrical obstruction is located in the central region of the flow field. With elapsed time, some bacteria attach on the circular surface (marked as red dots in Fig. 3B). The simulation shows more bacteria attached on the left side of the rectangular obstruction. Bacterial density decreases with increasing angle to the inflow direction. This is also consistent with the experimental observation.

We have confirmed velocity profiles of the fluid flow can change the distribution of attached bacteria. For further analysis of the inherent reason, the streamline in the rectangular channel is analyzed (Fig. 4A). In the entrance region, the streamline is dense since the velocity profile is not fully developed. The boundary layer, defined as fluid in the immediate vicinity of a bounding surface, is much thinner in this region. While in the central region, the streamline is sparse and parallel, leading to thicker boundary layer. The locomotion of bacterium in flow derives from two factors: the swimming of bacterium (including flagellar propulsion, Brownian motion and tumbling), and the non-slip movement with the ambient fluid. The bacterial swimming is dominant when the bacterium is in the boundary layer, since the fluid velocity perpendicular to the surface is negligible. In the entrance region, the boundary layer is thinner. Thus it is easier for the bacterium to swim across the fluid layer and attach on the substratum, leading to higher density.

The streamline over the cylindrical obstruction is plotted in Fig. 4B. On the left side of the obstruction, the streamline is denser compared to the entrance section in the rectangular channel. This facilitates the swimming of bacteria across the boundary layer and then attach on the surface. That is why the bacterial density at the location of $\theta = 0°$ is higher than the entrance section in the rectangular channel (344 vs. 199 cells/mm^2). Besides, the streamline reveals the boundary layer thickness at the location of $\theta = 45°$ and $\theta = 90°$ are close to each other, leading to similar bacterial densities which are 213 and 208 cells/mm^2, respectively. As a comparison, the boundary layer thickness at the location of $\theta = 135°$ is much larger, resulting in the lowest attached bacterial density.

We have stated that the locomotion of bacterium derives from two factors: bacterial swimming (including flagellar propulsion, Brownian motion and tumbling) and the motion with flow. The relative importance of the two factors can be evaluated by the Péclet number.

$$Pe = \frac{Lu}{D} \tag{15}$$

where L is the characteristic length, u is the local flow velocity, D is the mass diffusion coefficient for the bacteria (or the swimming velocity of the bacteria). Lower Pe values means higher swimming velocity of the bacteria and less time for the bacteria to reach the surface. In the boundary layer where the bacterial swimming is dominant, it is effective to enhance the bacterial attachment by reducing the boundary thickness. Fig. 4C is the Pe number for the bacterial locomotion in the rectangular channel. In the fully-developed section, there is a layer with low Pe number. While for the entrance section, this layer is much thinner, leading to more attached bacteria.

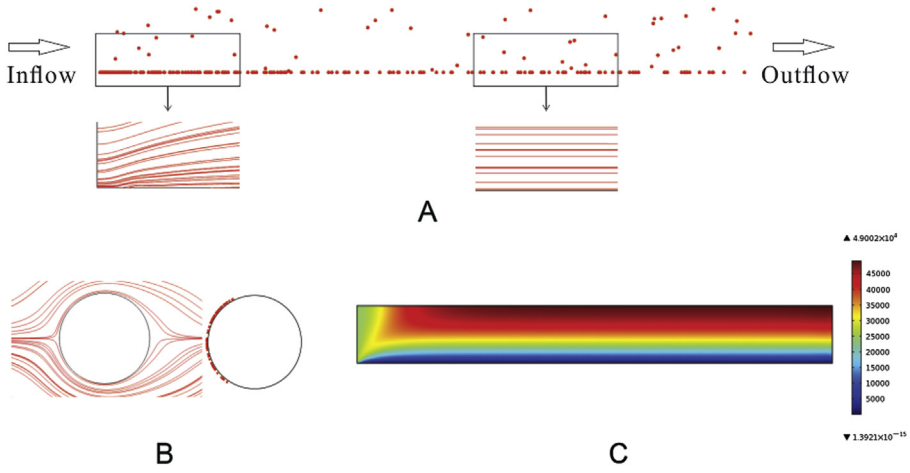

Fig. 4. (A) Attached bacteria distribution and streamline at the inlet and fully-developed section. (B) Attached bacteria distribution on the circular surface and the streamline over the obstruction (C) *Pe* number in the rectangular channel.

This analysis can be used as a guideline in the design of biological reactor. If more bacteria is desired to attach on the substratum, e.g. the biofilm reactor, it should be optimized with a lower *Pe* number near the substratum. And the boundary layer should be as thin as possible. This will enhance the bacterial attachment and biofilm formation. If biofilm is harmful in a certain circumstance, the reactor should be operated under a condition with higher *Pe* number near the surface, to minimize the attached bacteria. A new design of biological reactor can be verified by the mathematical model proposed in the present study, reducing the cost and attempt in the optimization.

Conflict of interest

The authors declare no conflict of interest.

Acknowledgments

The authors gratefully acknowledge the financial support from the National Natural Science Foundation of China (No. 51136007), the National Natural Science Funds for Distinguished Young Scholar (No. 51325602), the Research Project of Chinese Ministry of Education (No. 113053A) and the Natural Science Foundation of Chongqing, China (No. cstc2013jjB9004).

Transparency document

Transparency document related to this article can be found online at http://dx.doi.org/10.1016/j.bbrc.2015.04.089.

References

[1] X.b. Hu, et al., Characteristics of biofilm attaching to carriers in moving bed biofilm reactor used to treat vitamin C wastewater, Scanning 35 (5) (2013) 283–291.
[2] C.-L. Guo, et al., Enhanced photo-H2 production by unsaturated flow condition in continuous culture, Biotechnol. Lett. 37 (2) (2015) 359–366.
[3] Z. Hu, et al., Nitrogen removal with the anaerobic ammonium oxidation process, Biotechnol. Lett. 35 (8) (2013) 1145–1154.
[4] H.C. Berg, Random Walks in Biology, ix, Princeton University Press, Princeton, N.J, 1983, p. 142.
[5] Z. Cheng, et al., Bioaugmentation of a sequencing batch biofilm reactor with Comamonas testosteroni and Bacillus cereus and their impact on reactor bacterial communities, Biotechnol. Lett. 37 (2) (2015) 367–373.
[6] J. Seok, S. Komisar, Sequential kinetic parameter estimation of anaerobic fluidized bed bioreactor using an optimization technique, Biotechnol. Lett. 24 (19) (2002) 1579–1586.
[7] B.C. Dunsmore, C.J. Bass, H.M. Lappin-Scott, A novel approach to investigate biofilm accumulation and bacterial transport in porous matrices, Environ. Microbiol. 6 (2) (2004) 183–187.
[8] S. Woodcock, et al., Modelling the effects of dispersal mechanisms and hydrodynamic regimes upon the structure of microbial communities within fluvial biofilms, Environ. Microbiol. 15 (4) (2013) 1216–1225.
[9] J. Gray, G. Hancock, The propulsion of sea-urchin spermatozoa, J. Exp. Biol. 32 (4) (1955) 802–814.
[10] D. Katz, J. Blake, S. Paveri-Fontana, On the movement of slender bodies near plane boundaries at low Reynolds number, J. Fluid Mech. 72 (03) (1975) 529–540.
[11] R. Johnson, C. Brokaw, Flagellar hydrodynamics. A comparison between resistive-force theory and slender-body theory, Biophysical J. 25 (1) (1979) 113–127.
[12] H.C. Berg, E. coli in Motion. Biological and Medical Physics Series, xi, Springer, New York, 2004, p. 133, 1 col. plate.
[13] M.J. Kim, et al., Particle image velocimetry experiments on a macro-scale model for bacterial flagellar bundling, Exp. Fluids 37 (6) (2004) 782–788.
[14] E. Lauga, et al., Swimming in circles: motion of bacteria near solid boundaries, Biophysical J. 90 (2) (2006) 400–412.
[15] H. Berg, D. Brown, Chemotaxis in Escherichia coli analysed by three-dimensional tracking, 1972.